accuracy of the final models on the independent test dataset (Fig 3 bottom right). The resulting generalization error for optimal λ^* on left-out data had a mean of 0.181 across the 10 models and of 0.118 for phenotypic data alone, and the corresponding Pearson correlation coefficient between model prediction and the experimentally measured data was 0.54 (molecular and phenotypic) and 0.79 for the phenotypic data alone. The correlation was found to be higher in the later time points of molecular and phenotypic data. In particular, the Pearson correlation coefficient between predictions and measurements of the combined molecular and phenotypic data was 0.71 on the combined last three time points (24, 48, and 67 hours) and 0.74 for the last time point alone (S5 Fig). Hence, the inferred temporal model had the highest accuracy at the 67-hour time point. We conclude that the method for network modeling has a reasonably accurate predictive power, especially for predictions in the 24–67 hour range and that the models are useful for predicting the effects of new perturbations as hypotheses. Reasonable accuracy means that an affordable number of experiments would lead to a positively validated result (a 'hit') that can be advanced to pre-clinical investigation.

Analysis of network models. We used the optimal regularization parameter $\lambda^* = 3$ to infer 101 network models on all available data. To have reasonable diversity, the models were inferred without using prior information, i.e., known biological interactions. Several key model interactions agreed with interactions reported in the literature. The inferred effect of selected drugs on proteins (Fig 4) was in agreement with known drug–protein interaction patterns (e.g., MEKi inhibits the phorphorylation of ERK1/2 at T202/Y204 and RAFi inhibits MEK1/2 phorphorylation at S217/221) as well as unknown interactions (e.g., PKCi inhibits phorphorylation of CREB at S133). In addition, these model-derived drug–protein effects were in agreement with the observed drug effects from single-drug RPPA measurements (S2 Fig).

Saturation effects of drugs are taken into account by the model using the open parameter δ_i. For values of $0 < \delta_i < 1$, we have an almost linear drug effect; values of $\delta_i > 1$ do not result in any significant change as drug concentrations increase. For the case of PKC and SRC inhibitors, we find a δ_i in the linear range, i.e., that a doubling of the low dose results in almost the double response, while RAF and JNK inhibitors have almost reached saturation, i.e., no significant difference between the drug effect in low and high dose of the drugs (S3 Fig).

Predicted effect of drug perturbations and nomination of targets for drug testing. Using the 101 inferred network models, we predicted the phenotypic response (cell growth

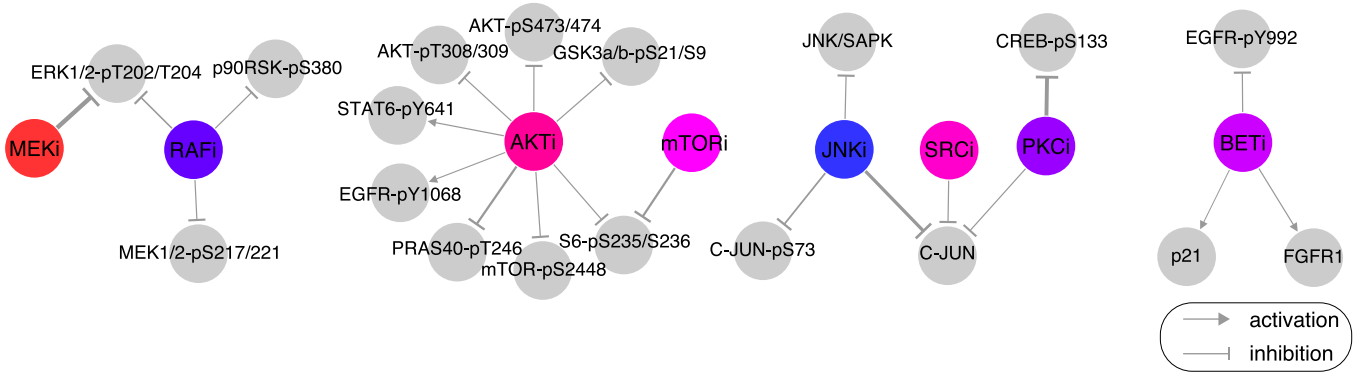

Fig 4. Model-inferred effect of drugs on proteins and phospho-proteins. The effect of drug treatment on (phospho-)protein levels is captured as edges between drugs (colored circles) and proteins (gray circles) in the model (represented by the drug–(phospo-)protein interaction strength d_{il} from Eq 2). Some of the edges are well known (e.g., MEKi inhibits ERK1/2-pT202/T204) and some appear to be novel or indirect (e.g., inhibitory effect of PKCi on CREB-pS133). Based on the distribution of edge values over the 101 network models, only the strongest drug–protein edges are displayed for visualization purposes (85th percentile for positive/activating interactions and 15th percentile for negative/inhibiting interactions, by absolute value).

https://doi.org/10.1371/journal.pcbi.1007909.g004